

# A surface-plasmon-resonance sensor based on photonic-crystal-fiber with large size microfluidic channels

PIBIN BING<sup>1\*</sup>, JIANQUAN YAO<sup>2, 3</sup>, YING LU<sup>2, 3</sup>, ZHONGYANG LI<sup>1</sup>

<sup>1</sup>Institute of Electric Power, North China University of Water Resources and Electric Power, Zhengzhou 450011, China

<sup>2</sup>The Institute of Laser and Opto-electronics, College of Precision Instruments and Opto-electronics Engineering, Tianjin University, Tianjin 300072, China

<sup>3</sup>Key Laboratory of Optoelectronics Information and Technical Science (Ministry of Education), Tianjin University, Tianjin 300072, China

\*Corresponding author: bing463233@163.com

A surface-plasmon-resonance (SPR) sensor based on photonic-crystal-fiber (PCF) with large size microfluidic channels is proposed. The size of the microfluidic channels with gold coating can be enlarged by reducing the number of the holes in the second layer, so the structure of the PCF is simple and easy to manufacture. It is propitious for metal coating and infiltration of microfluidic. The contact area of sample and metal film is increased, and the interface is closer to the core, so the energy coupling between the plasmon mode and the core-guided mode is easier. Numerical results indicate that the excitation of the plasmon mode is sensitive to the change of the refractive index of adjacent analyte. Sensitivity of the sensor is comparable to the ones of the best existing waveguide sensors. The amplitude resolution is demonstrated to be as low as  $3.3 \times 10^{-5}$  RIU, and the spectral resolution is  $5 \times 10^{-6}$  RIU (where RIU means the refractive index unit). The refractive index of microfluidic can be measured effectively.

Keywords: photonic-crystal-fiber, surface-plasmon-resonance, sensor, finite element method.

## 1. Introduction

It is well known that surface plasmon is extremely sensitive to the variation of the surrounding dielectric while propagating at the metal/dielectric interface, so surface-plasmon-resonance (SPR) has been widely implemented in sensing structures nowadays [1, 2]. Conventional SPR sensors based on optical fiber were proposed for a long time [3] and some have already been commercialized [4]. Recently, photonic-crystal-fibers (PCFs) present high-quality microfluidic channels that can be

controllably filled with ultrasmall volumes of analytes and can be mass produced. Owing to the channels proximity to the optical core, they can have good overlap with the optical mode of the fiber, making them a natural candidate for sensing schemes [5]. Furthermore, high pressure chemical deposition technique was demonstrated that could be used to uniformly coat the surface of the holes of a PCF with a variety of materials [6]. So, SPR sensor based on PCF has attracted considerable interest in research and development. Utilizing this sensor, the refractive index of the adjacent analyte can be retrieved either by measuring the transmission spectrum or by monitoring the transmitted power at certain wavelength as the analyte infiltrates into the metal-coated holes of the PCF [7].

HASSANI and SKOROBOGATIY introduced a concept of microstructured optical fiber (MOF, also called PCF) based SPR sensors [8, 9]. They analyzed design principles in detail for two different PCF structures with gold coating for biosensing applications. Both sensors show perfect performance in terms of sensitivity. Recently, XIA YU *et al.* proposed a selectively coated PCF based SPR sensor [10]. The sensor consists of selectively metal-coated air holes containing analyte channels, which effectively enhances the phase matching between the plasmon mode and the core-guided mode. The sensor design demonstrates that good refractive index sensitivity can be achieved.

In this paper, a SPR sensor based on PCF with large size microfluidic channels is proposed. The structure of the PCF is simple and easy to manufacture. It is propitious for metal coating and infiltration of microfluidic. The contact area of sample and metal film is increased, and the interface is closer to the core, so the energy coupling between the plasmon mode and the core-guided mode is easier. Finally, the refractive index of microfluidic can be measured effectively.

## 2. Simulated model

For an SPR sensor based on PCF, the most crucial requirement is phase matching between the plasmon and core-guided mode. The effective refractive index of the plasmon mode is mainly determined by the adjacent analyte, the coating metal and so on. We know that aqueous solution ( $n_a \approx 1.33$ ) is the most common analyte and gold is widely used as coating material for its excellent stable characteristics. The dielectric constant of gold is given by the Drude model which gives a good fit to the measurement results in the literature [11]. The effective refractive index of a core-guided mode is close to that of a core material. Usually, the background material of fiber is assumed to be silica glass ( $n_c \approx 1.45$ ). Accurately, the refractive index of the fiber is given by the Sellmeier dispersion relation [12].

The schematic diagram of the SPR sensor based on PCF is shown in Fig. 1. Actually, the structure with large size microfluidic channels can be regarded as a PCF that has a central air hole and two layers of symmetric hexagonally arranged holes. It should be noted that the holes in the second layer are removed alternately and the size for the holes left is enlarged. The central air hole is introduced into the fiber core to

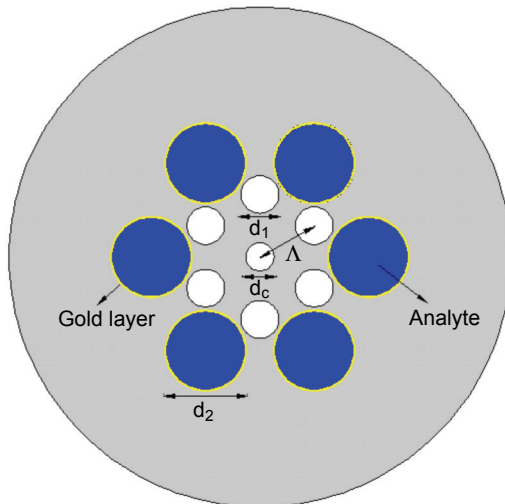


Fig. 1. Schematic design of the SPR sensor based on PCF.

reduce the effective refractive index of the core-guided mode. The lower effective refractive index of the core-guided mode could match with the plasmon mode well. On the other hand, the holes in the first-layer acting as a low effective refractive index cladding restrict the core-guided mode from propagating in the fiber core. Only small energy can infiltrate the gold-coated holes in the second layer through the aperture between the first-layer holes. The gold-coated holes acting as channels for the infiltration of the analyte in the second layer are considerably larger than those in the first layer. By introducing larger size holes in the second layer, the coating and infiltrating process become much more convenient in the microfluidic channels. Moreover, the energy coupling between the plasmon and core-guided mode is more efficient as the channels are close to the fiber core.

Compared with the structures reported [8–10], the dimensions are assumed to be unchanged. The pitch of the underlying hexagonal lattice is  $A = 2 \mu\text{m}$ , the diameters of the central and first-layer holes are  $d_c = 0.45A$  and  $d_1 = 0.6A$ , respectively. The holes shown as channels for analyte infiltration are coated with a 40 nm layer of gold in the second layer.

### 3. Results and discussion

The complex propagation constants of electromagnetic mode of the fiber sensor are investigated numerically via a finite element method (FEM) with perfectly matched layer (PML) boundaries. Assuming that the refractive index of the aqueous solution contained in the channels is  $n_a = 1.33$ . Figure 2 presents the power flow distribution of the sensor for the incident wavelength of  $0.57 \mu\text{m}$  and the diameter of the second-layer holes  $d_2 = 1.3A$ .

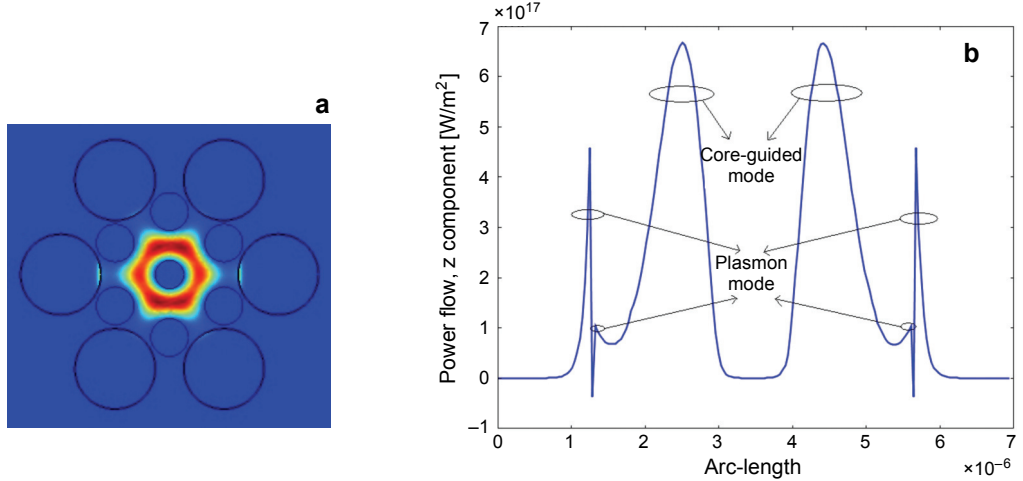


Fig. 2. The power flow distribution of the sensor: cross-section (a); across the fiber core and the microfluidic channels (b).

The phase matching between the plasmon and core-guided mode is possible as shown in Fig. 2. Most energy is confined in the fiber core by the cladding holes and only a part of energy penetrates into the gold-coated channels in the second layer to excite the plasmon mode. Figure 2b provides clearly the evidence for the existence of the plasmon mode. We can see that the internal and external gold-coated surfaces in the second-layer holes can both excite the plasmon mode. Furthermore, the plasmon mode excited by the internal surface is more intense. So, it is confirmed that the excitation of plasmon mode on the metal surface is more intense in the low refractive index interface than in the high refractive index interface. The excitation of the plasmon mode relates to the change of refractive index of the adjacent analyte. Based on the discussion above, we can conclude that the proposed structure is suitable for a sensor.

Dramatically, a part of the energy penetrates into the gold in the second-layer holes to excite the plasmon mode and the energy of the core-guided mode is dissipated. It can be assumed that the greatest loss of the core-guided mode is due to the excitation of the plasmon mode. We need to calculate the loss of the core-guided mode to determine the intensity of the excited plasmon mode. The loss in proportion to the imaginary part of the effective refractive index  $\alpha$  can be defined in decibels per meter as  $\alpha = 40\pi \text{Im}(N_{\text{eff}})/\lambda \ln(10)$ . Figure 3 shows the loss spectra of a core-guided mode for various diameters of the holes in the second layer  $d_2 = 0.8\Lambda, 1.0\Lambda, 1.2\Lambda, 1.3\Lambda$ . The diameters of the fiber core and first-layer holes equal  $d_c = 0.45\Lambda$  and  $d_1 = 0.6\Lambda$ , respectively.

From the figure we find that the frequency shift of the peak wavelength is from 0.57 μm for  $d_2 = 0.8\Lambda$  and 0.575 μm for  $d_2 = 1.0\Lambda, 1.2\Lambda$  to 0.57 μm for  $d_2 = 1.3\Lambda$ . The loss at 0.57 μm can be comparable to 0.58 μm in Ref. [9] and 0.56 μm in Ref. [10]

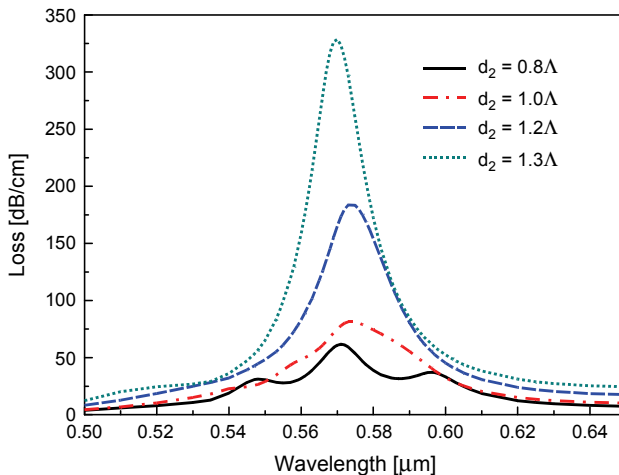


Fig. 3. Loss spectra of the core-guided mode for various values of the diameters of the second-layer holes  $d_2 = 0.8\Lambda, 1.0\Lambda, 1.2\Lambda, 1.3\Lambda$ .

for  $d_2 = 0.8\Lambda$ . This means that the resonance wavelength of the excited plasmon mode gives a good fit to the simulation results of the three similar structures. Moreover, we can observe an overall increase in the modal losses of a core-guided mode for the larger size holes in the second layer (as the holes in the first and second layer are tangential when  $d_2 = 1.4\Lambda$ ,  $d_2$  is increased from  $0.8\Lambda$  to  $1.3\Lambda$  in our simulation). The energy coupling between the plasmon and core-guided modes is more efficient as the channels are closer to the fiber core. The resonance strength of the excited plasmon mode is more sensitive to the change of the wavelength as the diameter of the second-layer holes is larger. So the sensor with large size microfluidic channels is worth recommending.

As we know, the plasmon resonance wavelength is extremely sensitive to the surrounding dielectric function of the aqueous solution. The loss spectra of the core-guided mode with different refractive index of the adjacent analyte are plotted in Fig. 4. The frequency shift of the peak loss is detected as the refractive index varying from  $0.57 \mu\text{m}$  for  $n_{\text{analyte}} = 1.33$ ,  $0.595 \mu\text{m}$  for  $n_{\text{analyte}} = 1.35$ ,  $0.625 \mu\text{m}$  and  $0.63 \mu\text{m}$  for  $n_{\text{analyte}} = 1.37$  to  $0.666 \mu\text{m}$  and  $0.676 \mu\text{m}$  for  $n_{\text{analyte}} = 1.39$ . At the same time, the plasmon mode is intensively excited as the refractive index of the adjacent analyte increases and the resonance peaks shift to longer wavelength area. It should be noticed that there are two resonance peaks as the refractive index of the adjacent analyte is larger than 1.37, which is because the higher order plasmon mode is excited. Furthermore, the intensity of the second resonance peak increases and then becomes the primary one as the refractive index of the adjacent analyte increases continuously.

There are two resonance peaks as the refractive index of the adjacent analyte is larger enough, as shown in Fig. 5. From the figure we can see that the second resonance appearing as the refractive index of the adjacent analyte is about 1.36. Furthermore,

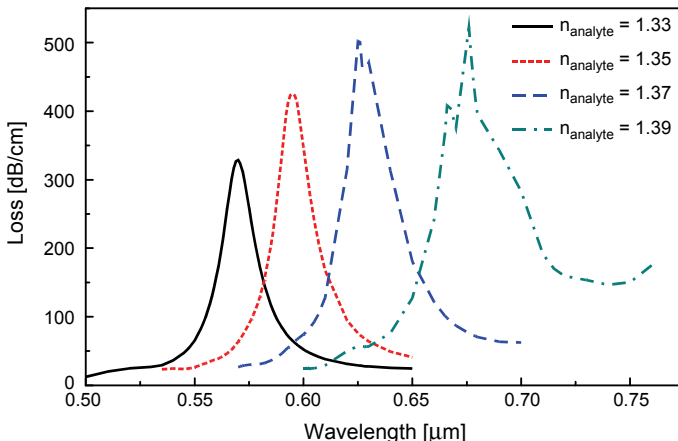


Fig. 4. Loss spectra with different refractive index of the analyte at 1.33, 1.35, 1.37 and 1.39.

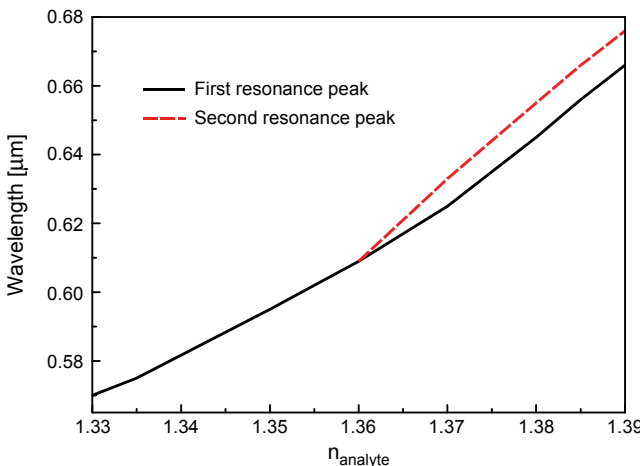


Fig. 5. The frequency shift of the resonance wavelength with the change of the refractive index.

the two resonance curves separate farther corresponding to the increase of the refractive index of the adjacent analyte, which can also be confirmed in Fig. 4. Therefore, the second resonance can be used as another parameter for sensing.

For a sensor, the most important parameters are sensitivity and resolution. Sensitivity means the variation in the ratio of the SPR resonance parameters (wavelength, amplitude, *etc.*) to the refractive index of the samples. Resolution is the minimum variation that the system can detect in the measured parameters of the sample volume. We can describe the sensitivity of the sensor by means of an amplitude (or phase) based method or wavelength interrogation method.

In amplitude based method, we can define  $\alpha(\lambda, n_a)$  to be the transmission loss of a core mode as a function of the wavelength and refractive index of analyte.

Assuming  $P_0$  to be the power launched into the fiber core mode, the power detected after propagation along the sensor with the length  $L$  will be  $P(L, \lambda, n_a) = P_0 \exp[-\alpha(\lambda, n_a)L]$ . A reasonable choice of sensor length falls into a subcentimeter range for the PCFs described in this paper and the corresponding sensor volume is then subnanoliter. So, one can express  $L = 1/\alpha(\lambda, n_a)$  and the amplitude sensitivity of the analyte refractive index change can be written as [9]:

$$S_A(\lambda)(\text{RIU}^{-1}) = \frac{\partial \alpha(\lambda, n_a)/\partial n_a}{\alpha(\lambda, n_a)} \quad (1)$$

In Figure 6, we describe the amplitude sensitivity of the sensor for  $d_2 = 1.3\text{\AA}$ . Maximum amplitude sensitivity of the PCF sensor with large size microfluidic channels for detecting changes in the aqueous analyte in the vicinity of  $0.6\text{\mu m}$  is  $300\text{ RIU}^{-1}$ , which means  $1300\text{ dB}\cdot\text{RIU}^{-1}$ . It can be assumed that a 1% change in the transmitted intensity can be detected reliably, which leads to the sensor resolution of  $3.3\times 10^{-5}\text{ RIU}$ , where RIU means the refractive index unit.

On the other hand, a wavelength interrogation method can also be used to calculate the sensitivity of the sensor. By detecting  $\Delta\lambda_P$  shift of the peak position of the resonant core mode loss for  $\Delta n_a$  change of the analyte refractive index, the spectral sensitivity in wavelength interrogation method can be expressed as [9]:

$$S_\lambda(\text{RIU}^{-1}) = \frac{\Delta\lambda_P}{\Delta n_a} \quad (2)$$

According to the results of the numerical calculation in Fig. 4, the interval distance enlarges as the refractive index of the adjacent analyte increases with the same margin. So the sensitivity of the sensor increases continuously and the maximal spectral resolution of the system is about  $2\text{\mu m/RIU}$ , which is  $5\times 10^{-6}\text{ RIU}$  with a demodulation

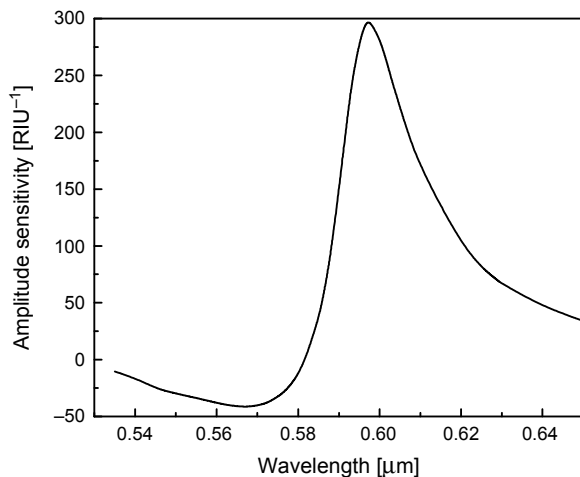


Fig. 6. Amplitude sensitivity of the sensor.

resolution of 10 pm from the spectrometer. Based on the discussion above, sensitivities of our sensors are comparable to the ones of the best existing waveguide sensors [13].

## 4. Conclusions

We have proposed a SPR sensor based on PCF with large size microfluidic channels. The plasmon on the surface of the gold-coated channels containing analyte can be intensively excited by the core-guided mode. By introducing the large size microfluidic channels, the metal coating and infiltration of microfluidic will be convenient. Moreover, the contact area of sample and metal film is increased, and the interface is closer to the core, so the energy coupling between the plasmon mode and the core-guided mode is easier. Numerical results indicate that the excitation of the plasmon mode is sensitive to the change of the refractive index of adjacent analyte. The resonance strength is more sensitive to the change of the wavelength as the diameter of the channels is larger (1.3 $\mu$ m). Compared with the previous structures reported, the sensor proposed in this paper gives higher sensing resolution. The detection limit of the amplitude based sensor for measuring changes in the aqueous analyte in the vicinity of 0.6  $\mu$ m is 300 RIU $^{-1}$ , assuming that a 1% amplitude change can be detected reliably, which leads to the sensor resolution of  $3.3 \times 10^{-5}$  RIU. The detection limit of the same sensor by spectral measurement is predicted to be 2  $\mu$ m/RIU, which is  $5 \times 10^{-6}$  RIU with demodulation resolution of 10 pm from the spectrometer.

*Acknowledgments* – This work was supported by the National Basic Research Program of China under Grant No. 2010CB327801.

## References

- [1] SLAVIK R., HOMOLA J., CTYROKY J., *Miniaturization of fiber optic surface plasmon resonance sensor*, Sensors and Actuators B **51**(1–3), 1998, pp. 311–315.
- [2] SCHMIDT M.A., PRILL SEMPERE L.N., TYAGI H.K., POULTON C.G., RUSSELL P.S.T.J., *Waveguiding and plasmon resonances in two-dimensional photonic lattices of gold and silver nanowires*, Physical Review B **77**(3), 2008, article 033417.
- [3] BYOUNGHO LEE, *Review of the present status of optical fiber sensors*, Optical Fiber Technology **9**(2), 2003, pp. 57–79.
- [4] BYOUNGHO LEE, SOOKYOUNG ROH, JUNGHYUN PARK, *Current status of micro- and nano-structured optical fiber sensors*, Optical Fiber Technology **15**(3), 2009, pp. 209–221.
- [5] WU D.K.C., KUHLMAY B.T., EGGLETON B.J., *Ultrasensitive photonic crystal fiber refractive index sensor*, Optics Letters **34**(3), 2009, pp. 322–324.
- [6] SAZIO P.J.A., AMEZCUA-CORREA A., FINLAYSON C.E., HAYES J.R., SCHEIDEMANTEL T.J., BARIL N.F., JACKSON B.R., DONG-JIN WON, FENG ZHANG, MARGINE E.R., GOPALAN V., CRESPI V.H., BADDING J.V., *Microstructured optical fibers as high-pressure microfluidic reactors*, Science **311**(5767), 2006, pp. 1583–1586.
- [7] HAUTAKORPI M., MATTINEN M., LUDVIGSEN H., *Surface-plasmon-resonance sensor based on three-hole microstructured optical fiber*, Optics Express **16**(12), 2008, pp. 8427–8432.

- [8] HASSANI A., SKOROBOGATIY M., *Design of the microstructured optical fiber-based surface plasmon resonance sensors with enhanced microfluidics*, Optics Express **14**(24), 2006, pp. 11616–11621.
- [9] HASSANI A., SKOROBOGATIY M., *Design criteria for microstructured-optical-fiber-based surface-plasmon-resonance sensors*, Journal of the Optical Society of America B **24**(6), 2007, pp. 1423–1429.
- [10] XIA YU, YING ZHANG, SHANSHAN PAN, PING SHUM, MIN YAN, LEVIATAN Y., CHANGMING LI, *A selectively coated photonic crystal fiber based surface plasmon resonance sensor*, Journal of Optics **12**(1), 2010, article 015005.
- [11] JOHNSON P.B., CHRISTY R.W., *Optical constants of the noble metals*, Physical Review B **6**(12), 1972, pp. 4370–4379.
- [12] RAJAN, SHARMA A.K., GUPTA B.D., *Fibre optic sensor based on long-range surface plasmon resonance: A theoretical analysis*, Journal of Optics A: Pure and Applied Optics **9**(7), 2007, pp. 682–687.
- [13] HOMOLA J., YEE S.S., GAUGLITZ G., *Surface plasmon resonance sensors: Review*, Sensors and Actuators B **54**(1–2), 1999, pp. 3–15.

Received September 12, 2011